

Bang-bang shortcut to adiabaticity in trapped-ion quantum simulators

S. Balasubramanian

Department of Physics, Massachusetts Institute of Technology, Cambridge, Massachusetts 02139, USA

Shuyang Han, B. T. Yoshimura, and J. K. Freericks

Department of Physics, Georgetown University, Washington, D.C. 20057, USA

(Received 27 September 2017; published 12 February 2018)

We model the bang-bang optimization protocol as a shortcut to adiabaticity in the ground-state preparation of a trapped-ion quantum simulator. Compared to a locally adiabatic evolution, the bang-bang protocol typically produces a lower ground-state probability, but its implementation is so much simpler than the locally adiabatic approach, that it can become a competitive choice to use for maximizing ground-state preparation in systems that cannot be solved with conventional computers. We describe how one can optimize the shortcut and provide specific details for how it can be implemented with current trapped-ion quantum simulators. However, when frustration is strong enough, no method appears to work well for adiabatic state preparation within the experimental time frames, and one must confront the issue of dealing with diabatic excitations within the simulation.

DOI: [10.1103/PhysRevA.97.022313](https://doi.org/10.1103/PhysRevA.97.022313)**I. INTRODUCTION**

There has been much recent progress in trapped-ion quantum simulation. Original experiments focused on adiabatic state preparation [1–3] of the transverse-field Ising model by initially orienting all of the spins along the field axis (in a large initial field) and then exponentially ramping the field to zero to prepare the ground state of the Ising model. Adiabatically preparing a complex quantum ground state is one of the crucial steps in many quantum computing algorithms and forms the cornerstone for adiabatic quantum computation. Unfortunately, when the system size was increased in experiments, and frustrated antiferromagnetic systems were examined, it became clear that there was a large amount of diabatic excitation [4]. This led to the study of excited states [4–7] and to a protocol that optimizes the field ramp with a locally adiabatic criterion [8]. In addition, other experimental situations were examined, such as Lieb-Robinson bounds [9,10] and higher-spin cases [11]. Currently, there are two foci for adiabatic state preparation: (i) Find shortcuts which will allow the original protocol to be achieved or (ii) use the diabatic excitations as a means to study low-energy excitations. Within the first category, recent work has found an exact shortcut for adiabatic state preparation [12,13] (at least for the nearest-neighbor transverse-field Ising model), but the multiple-spin interactions needed to accomplish this goal are too complicated to implement in the current generation of quantum simulators. In the second category, we already mentioned experimental [4,5,7] and theoretical [6] methods to produce or measure specific excitations. It is also possible, especially for ferromagnetic systems [14], for the diabatic excitations to resemble an equilibrium thermal state, which likely is related to the eigenstate thermalization hypothesis.

The bang-bang protocol has long been known within the field of quantum control as a useful optimization algorithm [15]. It invokes a control strategy similar to the algorithm employed with a thermostat, which sequentially turns the

climate control system fully on or fully off to maintain the temperature within a specified range. Here, it corresponds to quenching the magnetic field to an initial value, holding it for a fixed time, and then subsequently quenching it to zero. This protocol is illustrated schematically in Fig. 1(a), along with the more conventional locally adiabatic ramp [8] and the exponential ramp. The locally adiabatic ramp is determined by having uniformity in the diabatic excitations throughout the ramp *subject to the experimental limitation on the total time allowed for the experiment to run*. It strives to ramp the field quickly when the energy gap to the lowest coupled excited state is high, and more slowly when that gap is small. However, determining the ramp profile requires explicit knowledge of the excitation energy to the first coupled excited state as a function of magnetic field. While this can be found experimentally, utilizing different methods for small systems [5–7], it is a difficult procedure to carry out for large systems that have significant frustration. This effectively rules out the usefulness of such an approach for quantum simulators that examine frustrated systems, which cannot already be simulated by conventional computers. The bang-bang protocol is much simpler and can be easily employed on large frustrated systems, as long as one can determine the probability that the system remains in the ground state. It is motivated, in part, from a mathematical proof which says the most adiabatic ramp starts and ends with the flattest field profile [16]; the bang-bang approach carries this functional form to its extreme limit by employing a quench after a hold time. It works by projecting the initial state onto a collection of eigenstates at an intermediate field, allowing those states to evolve in the constant field until the projection onto the field-free ground state is maximized, and subsequently quenching to zero field, while projecting the final state onto the field-free eigenstates. It is not clear whether waiting longer times will necessarily improve the bang-bang shortcut. But, our results certainly suggest that improvements in the final ground-state probability can occur if one runs the

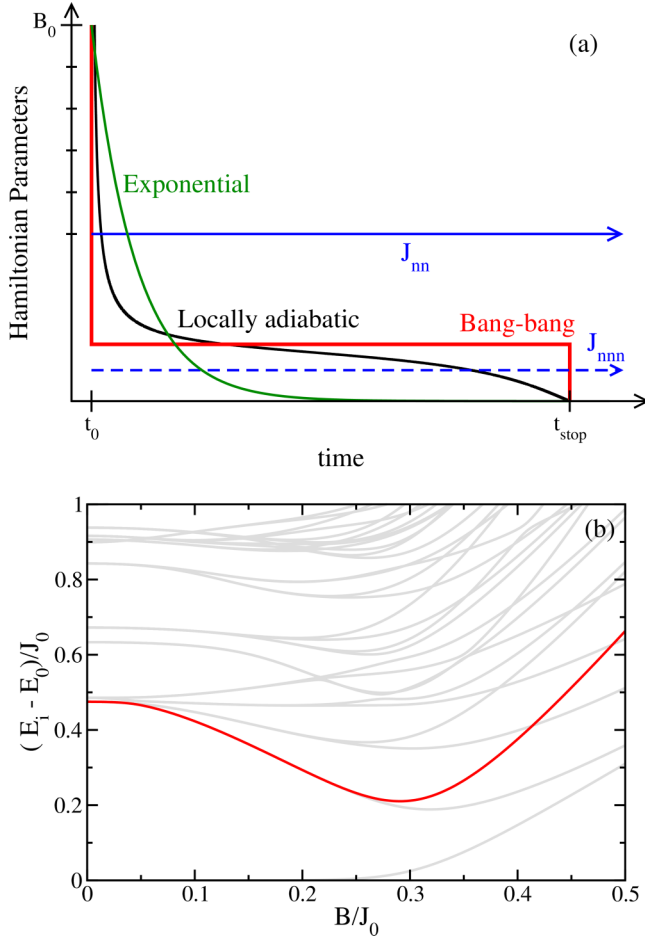


FIG. 1. (a) Comparison of the different ramp protocols. The magnetic interactions are held fixed, while the field is ramped from an initial value about five times the average nearest-neighbor exchange to zero. Three ramp profiles are shown—the locally adiabatic ramp, which strives to have a uniform rate of diabatic excitation throughout the ramp, the bang-bang protocol, with sharp steps, and the exponential ramp with a time constant one fifth of the experimental run time. (b) The low-lying spectra of an $N = 10$ Ising chain with spin-spin interactions for the trap used in Ref. [4] vs the ground-state energy as a function of the magnetic field (here, the exchange coefficients decay with an approximate power law of $\alpha = 1.05$). Since the transverse-field Ising model has both spatial parity and spin-reflection parity, the red line denotes the lowest-energy state that is coupled to the ground state and hence plots $\Delta(B)$, as described in the text.

experiment over a longer period of time. It is likely that this is intimately related to quantum speed limits [17], as recently discussed by Campbell and Deffner, who relate the energy cost associated with an adiabatic shortcut to quantum speed limits via operator norms [18].

The results in Sec. III show that the bang-bang protocol appears to work better the longer range the interactions are. Moreover, as the power α for the decay of the spin-spin coupling increases, we find the bang-bang protocol deviates more and more from the locally adiabatic approach. Nevertheless, because of its simplicity in implementation, it remains an attractive alternative for the temporal profile of the field

ramp. In addition, it can provide a different perspective for understanding diabatic excitations within quantum simulators.

In Sec. II, we discuss the formalism for this work, the results are presented in Sec. III, and the conclusions follow in Sec. IV.

II. FORMALISM

The Hamiltonian for the transverse-field Ising model is

$$\mathcal{H}(t) = - \sum_{i,j=1}^N J_{ij} \sigma_i^x \sigma_j^x - B^z(t) \sum_{i=1}^N \sigma_i^z. \quad (1)$$

Here, σ_i^r is the Pauli spin matrix (with eigenvalues ± 1 and with $r = x, y$, or z denoting the spatial direction of the Pauli matrix) at lattice site i , $B^z(t)$ is the time-dependent transverse field, and N is the number of spins in the lattice; we work in units with $\hbar = 1$ and simulate the transverse-field Ising model in a linear Paul trap. Experimentally, the model is generated by using the clock states of the $^{171}\text{Yb}^+$ ion as the spin-up and spin-down states and driving the system with a laser-induced spin-dependent force. This is achieved by employing both red and blue detuned laser beams from the carrier transition which induce a σ^x operation on the hyperfine states, whose strength is proportional to the phonon coordinate at lattice site i . Integrating out the phonons, under the assumption that they are only virtually occupied during the experiment, yields the following static spin-exchange coefficients—after averaging over their time dependence—[19] (we use conventional frequency units for all parameters),

$$J_{ij} = \Omega^2 \nu_R \sum_{m=1}^N \frac{b_i^m b_j^m}{\mu^2 - \omega_m^2}. \quad (2)$$

We employ the experimental parameters from Ref. [4] where $\Omega = 600$ kHz is the Rabi frequency, $\nu_R = \hbar/(M\lambda^2) = 18.5$ kHz is the recoil energy of a $^{171}\text{Yb}^+$ ion (with \hbar being Planck's constant, M the mass of the ion, and $\lambda = 355$ nm the wavelength of the laser light). In addition, b_i^m is the value of the orthonormal eigenvector at the i th ion site of the m th transverse normal mode for the N -ion chain, ω_m is the corresponding normal-mode frequency, and μ is the detuning of the laser from the transverse center-of-mass mode (which we take to be $\mu = 4.8$ MHz + 111.7 kHz). We let $J_0 < 0$ denote the average nearest-neighbor spin-spin interaction for the antiferromagnetic case. The transverse center-of-mass mode is fixed at 4.8 MHz. The axial center-of-mass mode has its frequency adjusted from 355 kHz to 1.25 MHz, corresponding to a nearest-neighbor exchange interaction which is near 1 kHz ($|J_0| \approx 1$ kHz); the exchange coefficients decay with an approximate power law $J_{ij} \approx J_0/|R_i - R_j|^\alpha$ (with R_i the equilibrium position of the i th ion) that ranges from $0.5 < \alpha < 2$ (where a smaller trap frequency corresponds to a larger power law). As the power law becomes more uniform ($\alpha \rightarrow 0$), the number of ion sites where the linear chain is stable decreases. Thus, we only present data for smaller ion number cases in that regime (see below for details). For large α , we have to decrease the frequency to unphysically low values to use the same scheme to adjust the power law; furthermore, because the bang-bang protocol does not work well there, we do not show or discuss those data in detail here.

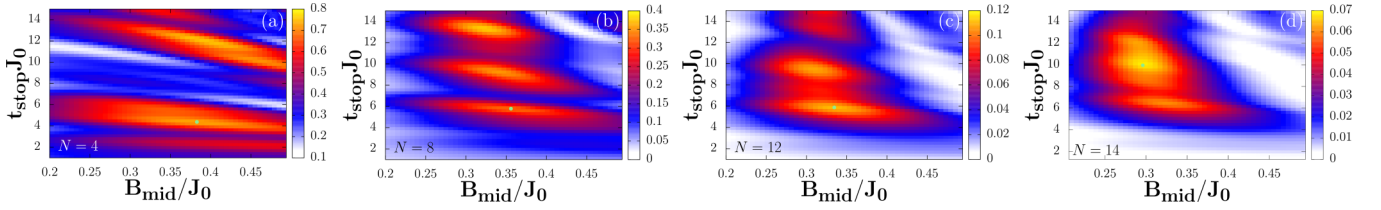


FIG. 2. False-color plots of the ground-state probability for the bang-bang shortcut to adiabaticity as a function of hold time and quench magnetic field for $\alpha = 1.05$. Different panels correspond to different N values: (a) $N = 4$; (b) $N = 8$; (c) $N = 12$; and (d) $N = 14$. Note the interesting plateaus that form, and remain at specific times for a range of magnetic quench fields. The light green circle marks the optimized value for the time interval of $t_{\text{exp}} < 6$ ms. Note that the false-color scale changes in each panel, as indicated on the accompanying legend.

For the bang-bang optimization, the time evolution of the wave function is trivial to calculate. Each quench is handled by the sudden approximation. Both the quench field and the hold time are varied to optimize the final ground-state probability. An experimental implementation requires determining the probability to be in the final ground state to carry out the optimization. This might be difficult to achieve if the ground state is not known *a priori*, but techniques do exist that allow for an estimation of ground-state probabilities [20] without requiring knowledge of the ground-state wave function. Note that since we want to pick the B field to be near the region of minimal gap, we typically choose values between $0.2 \leq B_0/|J_0| \leq 0.5$ when optimizing the protocol.

The locally adiabatic ramp is significantly more complicated to determine [11]. We start by calculating the excitation spectra $\Delta(B) = E_{\text{lex}} - E_{\text{g.s.}}$ for the first coupled excited state relative to the ground state (which can only be done if the system can be solved on a conventional computer; see Fig. 1). Then we determine the adiabaticity parameter γ from the relation [8] $\gamma = t_f / \int_0^{B_0} dB / \Delta^2(B)$, where $B_0 = 5|J_0|$ is the initial magnetic field and t_f is the total experimental time for the ramp. Note that because the initial state corresponds to the ground state for $B \rightarrow \infty$, the locally adiabatic protocol also starts with a magnetic field quench. With the adiabaticity parameter determined, the magnetic field ramp $B^z(t)$ is found by solving the first-order differential equation $dB^z(t)/dt = \Delta^2[B^z(t)]/\gamma$. We then evolve the wave function with the time-dependent field ramp by employing the Crank-Nicolson algorithm [21] employing a step size that is small enough. This method is also used for the exponential ramp.

The initial state for both cases is the state where the spins are completely aligned with the field, corresponding to $B^z \gg |J_0|$. However, the field ramp always starts with an initial field that is much lower than this: It is equal to $5|J_0|$ for the locally adiabatic ramp and is often much smaller for the bang-bang shortcut.

III. RESULTS

We choose the total experimental run time to be 6 ms—this is key for any realistic discussion of experiments, because this time is far too short to achieve adiabatic state preparation for all but the smallest systems. However, this time is somewhat longer than current experiments (which ran on the order of 2.4 ms [4]), even though it is certainly within reach with available technology. Moreover, it is certainly long enough that it allows us to compare the results of the bang-bang shortcut

to adiabaticity to the locally adiabatic ramp for chain sizes up to $N = 14$. We adjust the power law for the different cases by modifying the ratio of the trap frequencies, as is commonly done in experiment. This means we cannot examine as large systems for the smaller powers of α , because they become unstable, but it does allow us to otherwise compare different systems on the same footing.

We start by considering an intermediate power-law range, where the exchange couplings decay as a power law of approximately $\alpha = 1.05$. In Fig. 2, we show false-color images of the probability to be in the final ground state after the bang-bang shortcut for a given quench field (horizontal axis) and a given hold time (vertical axis). Note that there are high probability plateaus (primarily red and orange) and that the plateaus remain over a wide range of varying N in Figs. 2(a)–2(d). We use the word “plateau” due to the long flattened red regions in Fig. 2; the optimal probability is at the peak of this plateau region. As the system size increases, these plateaus are pushed upwards to longer hold times, and the area decreases, but they remain robust for a wide range of parameters—this is the key behind the ease in optimizing the bang-bang shortcut. Note how the red and orange plateaus lie in about the same location as the size of the system increases. This structure arises from the relationship between the eigenstates of the target final system ($B = 0$) and of the intermediate system ($B \approx J_0$) which necessitates a finite time evolution to maximize the amplitude of the target ground state in the eigenbasis of the intermediate system. (An analogy to this is inserting a polarizer at an angle θ between a pair of perpendicular polarizers as a light transmission device—one can never fully transmit the light, but placing the third polarizer at $\theta = 45^\circ$ will optimize the transmission.) The requirement that the hold time moves to longer times as N increases must be related to the quantum speed limit [17].

In Fig. 3, we plot vertical cuts through the false-color plots that show the final ground-state probability for the bang-bang shortcut at the optimal quench field near 6 ms for different power laws of the spin-spin exchange parameters. One notes that the stability of the plateaus is robust and does not depend strongly on the exponent of the decay of the exchange interactions, because the peaks occur at nearly the same time and have nearly the same magnitude for different power laws. One can also clearly see that as N increases, the plateaus at smaller hold times disappear, but the ones at higher hold times remain robust. These plateaus show that there are optimal quench fields and hold times for the bang-bang protocol, so it works better than some random choice of quench field and hold time. But in cases where the plateaus are broad, the

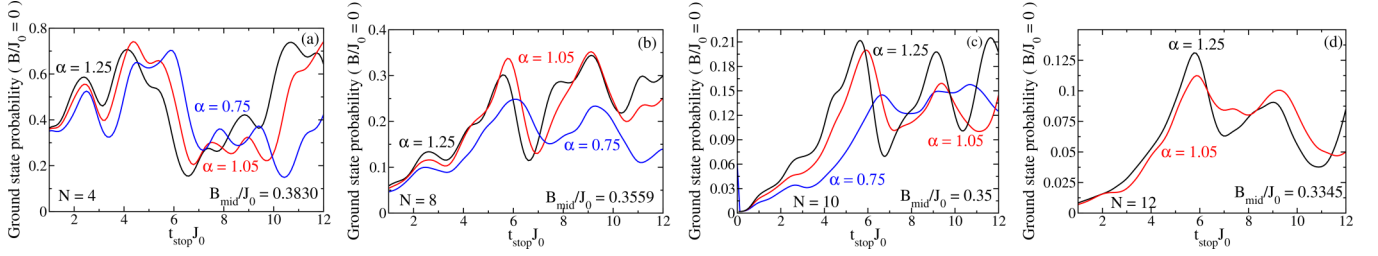


FIG. 3. Vertical cuts (perpendicular to the plateaus) through the false-color optimization plots for the bang-bang shortcut with three different power laws for the exchange coefficients: $\alpha = 0.75$, 1.05 , and 1.25 . Different panels correspond to different size ion chains: (a) $N = 4$; (b) $N = 8$; (c) $N = 10$; and (d) $N = 12$ (only the larger two power laws are stable here).

optimization does not depend strongly on the field or hold time, and the bang-bang approach becomes robust for a wide range of choices. As the size of the chain increases, and the magnetic frustration becomes stronger, one inevitably needs to go to longer hold times to achieve higher ground-state probabilities.

We also examined similar behavior for $\alpha = 0.5$ ($N_{\max} = 8$), $\alpha = 0.75$ ($N_{\max} = 10$), $\alpha = 1.25$ ($N_{\max} = 15$), $\alpha = 1.5$ ($N_{\max} = 12$), $\alpha = 2$ ($N_{\max} = 12$), $\alpha = 2.5$ ($N_{\max} = 12$), and $\alpha = 3$ ($N_{\max} = 12$). In all cases, we find that the bang-bang protocol produces similar stability plateaus as found for the $\alpha = 1.05$ case (for $\alpha \geq 1.5$, we stopped our calculations at $N_{\max} = 12$ because the bang-bang approach was not so competitive with the locally adiabatic ramp; for smaller α , we stopped at the given N_{\max} values because the chain became unstable due to the zigzag transition). Thus, the appearance of stable plateaus seems to be a universal feature of the bang-bang protocol, which explains its broad applicability. We find that the bang-bang protocol worked better for the smaller powers of α , as we show in the following series of figures (see Fig. 4).

One can see that the locally adiabatic ramp usually does better than the bang-bang shortcut for shorter-range couplings, but in some cases, the bang-bang approach is superior. In all cases, the bang-bang approach performs better than an exponential ramp, which is the most common experimental choice and the only other choice one can make if knowledge of the excitation gap is not known beforehand. Note, however, that even though the locally adiabatic ramp can outperform the bang-bang protocol most of the time, it requires detailed knowledge of the coupled energy spectrum and therefore becomes problematic to use for highly frustrated experimental

systems or for systems with large numbers of ions. The bang-bang protocol then emerges as a superior alternative to exponential ramping, especially for systems where one wants to perform fast prototyping. In particular, the fact that the bang-bang protocol does surpass the locally adiabatic protocol for some cases, provides an explicit counterexample to the conjecture that the locally adiabatic ramp is the optimal ramp for minimizing diabatic excitation [8].

IV. CONCLUSIONS

We examined the possibility of using a bang-bang shortcut to adiabaticity in trapped-ion quantum simulation as a way to optimize the ground-state probability for adiabatic state preparation. While we were not always able to produce better results than the locally adiabatic technique, the ease of implementing this protocol makes it a promising method for future experiments. We found that interesting stable plateaus formed in the plot of the final ground-state probability as a function of the quench field and the hold time. This illustrated not only why the bang-bang approach works but also showed that one needs to go to longer times for larger systems to be able to continue to optimize the ground-state probability. The plateaus also indicate that experimental optimization with the bang-bang approach is relatively simple—one picks a reasonable quench field on the order of J and varies the hold time to find the peak of the plateau. Then one varies the magnetic field in the vicinity of the optimal hold time. Because the plateaus occur at roughly the same hold time, one does not need to optimize over the magnetic field and the hold time simultaneously, but

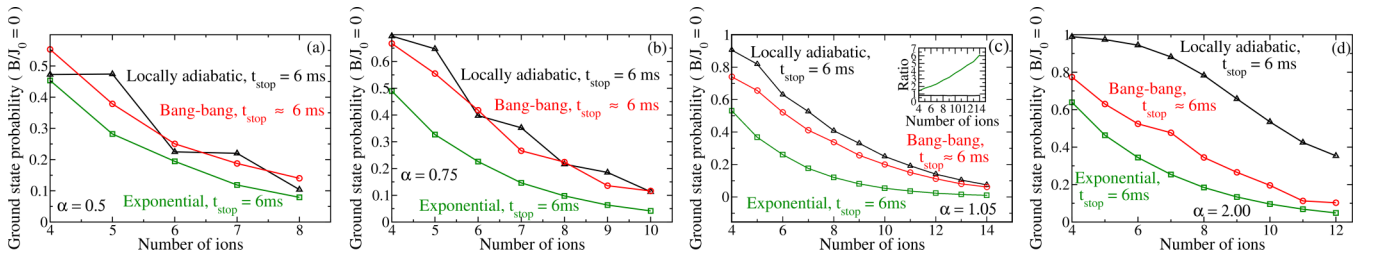


FIG. 4. Comparison of the final ground-state probability for the bang-bang shortcut vs the locally adiabatic ramp vs the exponential ramp. The horizontal axis is the number of ions in the chain. (a) is for the case $\alpha = 0.5$, where the bang-bang protocol occasionally beats the locally adiabatic one. This also holds for (b) with $\alpha = 0.75$. (c) is for $\alpha = 1.05$. In that panel, the inset is the ratio of the ground-state percentage for the bang-bang shortcut to the locally adiabatic ramp (black) and to the exponential ramp (green). One can clearly see that the bang-bang shortcut produces about 80% of the locally adiabatic probability for the ground state and it does not appear to improve as the number of ions increases. (d) shows the case $\alpha = 2$, where the bang-bang protocol always beats the exponential ramp, but lags significantly behind the locally adiabatic ramp. This same situation holds for larger α (not shown here). The lines are guides to the eye.

instead can alternate between optimizing over the field and the hold time. This speeds up the optimization procedure roughly quadratically, so that one rapidly settles in on the optimal field and hold time.

In general, our results also indicate that when a system has significant frustration, none of these techniques can maintain a high probability in the ground state—thus it is more useful to consider working with the diabatic distribution of excited states that ensues. In some cases, these distributions can closely mimic thermal distributions [14], but this does not often occur for frustrated spin systems. One advantage of this is with regards to phonon creation, since the continuous change in time of the Hamiltonian with the locally adiabatic ramp or the exponential ramp is likely to create more phonons [as quantitatively determined by the magnitude of $\int dt B^z(t)$ [22]].

We hope that experimentalists will consider employing quantum control ideas such as the bang-bang shortcut within

their experiments in the near future as they can be used to gain an even better understanding of how these quantum simulators work. In addition, whenever the bang-bang optimization occurs at a shorter time than the locally adiabatic ramp, then the experiment will have less decoherence, which can be another factor that is important in optimizing the state preparation, but is one that we do not model in this work.

ACKNOWLEDGMENTS

We acknowledge useful discussions with Adolfo del Campo. This work was supported by the National Science Foundation under Grants No. PHY-1314295 and No. PHY-1620555. J.K.F. was also supported by the McDevitt bequest at Georgetown University. B.T.Y. was also supported by the Achievement Rewards for College Scientists Foundation.

-
- [1] K. Kim, M.-S. Chang, S. Korenblit, R. Islam, E. E. Edwards, J. K. Freericks, G.-D. Lin, L.-M. Duan, and C. Monroe, *Nature (London)* **465**, 590 (2010).
 - [2] R. Islam, E. E. Edwards, K. Kim, S. Korenblit, C. Noh, H. Carmichael, G.-D. Lin, L.-M. Duan, C.-C. J. Wang, J. K. Freericks, and C. Monroe, *Nat. Commun.* **2**, 377 (2011).
 - [3] E. E. Edwards, S. Korenblit, K. Kim, R. Islam, M.-S. Chang, J. K. Freericks, G.-D. Lin, L.-M. Duan, and C. Monroe, *Phys. Rev. B* **82**, 060412(R) (2010).
 - [4] R. Islam, C. Senko, W. C. Campbell, S. Korenblit, J. Smith, A. Lee, E. E. Edwards, C.-C. J. Wang, J. K. Freericks, and C. Monroe, *Science* **340**, 583 (2013).
 - [5] C. Senko, J. Smith, P. Richerme, A. Lee, W. C. Campbell, and C. Monroe, *Science* **345**, 430 (2014).
 - [6] B. Yoshimura, W. C. Campbell, and J. K. Freericks, *Phys. Rev. A* **90**, 062334 (2014).
 - [7] P. Jurcevic, P. Hauke, C. Maier, C. Hempel, B. P. Lanyon, R. Blatt, and C. F. Roos, *Phys. Rev. Lett.* **115**, 100501 (2015).
 - [8] P. Richerme, C. Senko, J. Smith, A. Lee, S. Korenblit, and C. Monroe, *Phys. Rev. A* **88**, 012334 (2013).
 - [9] P. Richerme, Z.-X. Gong, A. Lee, C. Senko, J. Smith, M. Foss-Feig, S. Michalakakis, A. V. Gorshkov, and C. Monroe, *Nature (London)* **511**, 198 (2014).
 - [10] P. Jurcevic, B. P. Lanyon, P. Hauke, C. Hempel, P. Zoller, R. Blatt, and C. F. Roos, *Nature (London)* **511**, 202 (2014).
 - [11] C. Senko, P. Richerme, J. Smith, A. Lee, I. Cohen, A. Retzker, and C. Monroe, *Phys. Rev. X* **5**, 021026 (2015).
 - [12] A. del Campo, M. M. Rams, and W. H. Zurek, *Phys. Rev. Lett.* **109**, 115703 (2012).
 - [13] B. Damski, *J. Stat. Mech.: Theor. Exp.* (2014) P12019.
 - [14] M. H. Lim, B. T. Yoshimura, and J. K. Freericks, *New J. Phys.* **18**, 043026 (2016).
 - [15] L. Viola and S. Lloyd, *Phys. Rev. A* **58**, 2733 (1998).
 - [16] A. T. Rezakhani, A. K. Pimachev, and D. A. Lidar, *Phys. Rev. A* **82**, 052305 (2010).
 - [17] K. Bhattacharyya, *J. Phys. A: Math. Gen.* **16**, 2993 (1983).
 - [18] S. Campbell and S. Deffner, *Phys. Rev. Lett.* **118**, 100601 (2017).
 - [19] S.-L. Zhu, C. Monroe, and L.-M. Duan, *Phys. Rev. Lett.* **97**, 050505 (2006).
 - [20] B. Yoshimura and J. K. Freericks, *Front. Phys.* **3**, 85 (2015).
 - [21] J. Crank and P. Nicolson, *Proc. Cambridge Philos. Soc.* **43**, 50 (1947).
 - [22] C.-C. J. Wang and J. K. Freericks, *Phys. Rev. A* **86**, 032329 (2012).